ISBN: 978-3-95450-231-8 ISSN: 2673-5490 doi: 10.18429/JACoW-IPAC2023-WEPA150

DEVELOPMENT AND CHARACTERISATION OF ADVANCED COATINGS FOR HIGH ENERGY PHYSICS APPLICATIONS

A. T. Perez Fontenla†, C. P. A. Carlos, S. Leith, A. Moros, S. Pfeiffer, E. Rodriguez Castro, G. Rosaz, CERN, Geneva, Switzerland

Abstract

The Future Circular Collider (FCC) study develops the technologies for next generation high performance particle colliders and accelerating structures. It places high requirements on the performance of Superconducting Radio Frequency (SRF) cavities used to accelerate the particle beams. While niobium (Nb)-coated copper (Cu) cavities are being considered for FCC-ee, alternative superconducting materials like A-15 intermetallic type II superconductor Nb_3Sn are investigated in view of considerably reducing the energy consumption of such a large machine.

Nb/Cu cavities produced by DC magnetron sputtering (DCMS) were successfully deployed at CERN for LEP-II, LHC and HIE-ISOLDE. Nonetheless, this technology exhibited a behaviour termed Q-slope – strong degradation of the cavity's quality factor with increasing accelerating gradients – which was correlated to defects within the deposited layer. The use of High Power Impulse Magnetron Sputtering (HiPIMS), a distinct coating method that enables energetic condensation, has been shown to result in the desired densification of thin Nb and Nb_3Sn films during growth compared to films deposited by DCMS and RF performances with residual surface resistances similar to those of the state-of-the-art, with significant Q-slope mitigation.

Gaining understanding on the deposition parameters effect on the microstructural and mechanical properties is essential for improving the RF performance of these films. This work focuses on Nb_3Sn films deposited on Cu, which show a systematically lower critical temperature at a given composition compared to the reference data of Nb3Sn bulk. The study places special attention on interlayer characteristics to prevent volume diffusion of the Cu substrate during film deposition and/or subsequent thermal cycles.

INTRODUCTION

Previous studies have shown that Cu-Nb_3Sn interdiffusion at the interface can be harmful, and a possible solution is the use of a diffusion barrier to limit Cu mobility [1] [2]. However, the literature reports evidence of Cu penetrating through a metal layer without reacting with it, with short-circuit diffusion being the dominant transport mechanism.

Therefore, in order to ensure optimal barrier performance, it is crucial to consider not only the material composition of the barrier, but also its deposition method and associated parameters. Tantalum (Ta) is a refractory metal that is frequently utilized as a solid-state diffusion barrier in Metal-Oxide-Silicon (MOS) devices. Various Ta-based configurations are employed to separate the silicon and Cu metallization layers.

† ana.teresa.perez.fontenla@cern.ch

The effect of the deposition parameters on Ta and Nb_3Sn layers are closely examined in the present study using advanced electron microscopy tools and techniques such as Focused Ion Beam-Scanning Electron Microscope (FIB-SEM) and high-sensitivity Energy-Dispersive X-ray Spectroscopy (EDS) as well as diffraction techniques like Grazing Incident X-Ray Diffraction (GI-XRD) and Electron Backscattered Diffraction (EBSD), to gain insight into microstructural characteristics, phase evolution or stress kept within the films. Additional investigation of the Ta barrier elastic properties via instrumented nano-indentation complete the work.

EXPERIMENTAL WORK

Samples

The present investigation focuses on the four samples included in Table 1. The substrate used is in all cases Cu-OFE (20 minutes of SUBU [3] treatment). Both Ta and Nb_3Sn coatings were completed using bipolar HiPIMS [4] with a target to substrate distance of 100 mm and for the latest one an enriched Nb:Sn target with an atomic % ratio of 73:27 was employed.

Table 1: Samples and Coating Process Information

Sample	Layer/s	Temperature (°C)	Coating duration (Min.)
A	Ta	140	40
B	Ta	750 + 750	40 + 45
C	Ta+ Nb_3Sn	175 + 750	40 + 120
D	Ta + Nb_3Sn	750 + 750	85 + 120

The Ta layers were deposited using krypton pressure of $1x10^{-3}$ mbar, 350 W average power and 50 V positive pulse [5], while the Nb_3Sn layers used the same parameters with a higher deposition pressure of $2.5x10^{-2}$ mbar.

Samples A and B were coated with a single ~ 800 nm Ta layer. Sample A was coated without heating of the substrate holder and the temperature indicated is the final temperature reached during coating as a result of the plasma heating. Sample B on the other hand was coated at 750 °C and then post-coating annealed at the same temperature for 45 min. Samples C and D, each coated with an equivalent Ta layer to samples A and B respectively, were subsequently coated with a ~ 3 µm Nb_3Sn film at 750 °C, in order to form the A-15 phase during the deposition process.

ISBN: 978-3-95450-231-8 ISSN: 2673-5490 doi: 10.18429/JACoW-IPAC2023-WEPA150

Nb_3Sn Coating Homogeneity

The surface aspect and homogeneity of the Nb_3Sn films has been evaluated by field emission gun (FEG) SEM Sigma 500 from Zeiss and EDS conventional analysis. Representative SEM-micrographs are shown in Fig. 1.

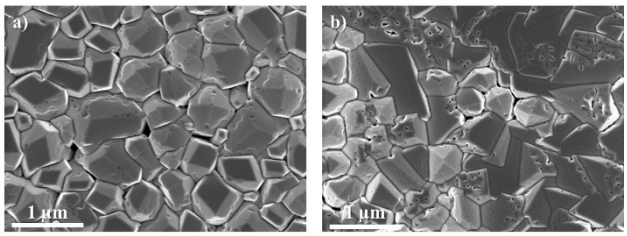

Figure 1: Surface SEM images on a) sample C and b) sample D.

The Nb_3Sn coated samples presented similar crystallites size and morphology at high magnification. When inspected using a larger field of view, circular features of different diameter appear randomly distributed all over the surface in sample C. Secondary electron (SE) image on a representative site is displayed in Fig. 2 a). Elemental mapping was performed on the same site with the help of the high sensitivity 100 mm² X-Max Extreme EDS detector from Oxford Instruments and is included in Fig. 2 b). The image provides a clear idea of the features size and the Cu presence (orange) against the greenish background corresponding to the Nb_3Sn layer.

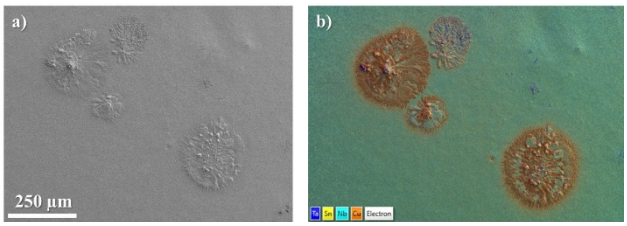

Figure 2: Features observed in sample C a) SE micrograph and b) EDS elemental map.

One of those features was studied through the layers thickness via FIB milling on a XB540 FIB from Zeiss. The FIB cross-sectional view is shown in Fig. 3. The Ta layer uniformly covers the Cu substrate without apparent defects or discontinuities. The Nb_3Sn crystallites appear disconnected at the upper region, surrounded by a Cu rich phase that is thicker at the centre and propagates laterally at approximately half of the layer thickness.

Sample D appears to have a more uniform Nb_3Sn layer when viewed from a morphological and compositional perspective, with no visible features. This could be attributed to the higher temperature reached during the Ta layer deposition and subsequent annealing, which is the only difference compared to the defective sample.

Characterization of the Ta Interlayers

Ta layers deposited with same parameters as samples C and D are compared from cross section and top view in Fig. 4. Both samples exhibit columnar grains with their longer axis perpendicular to the Cu-Ta interface. It is evident that the grains in sample B are larger than in sample A and it was confirmed by EBSD grain size analysis using a Nordlys detector from Oxford Instruments. The averaged diameter of the grains was estimated to be 170 nm ± 50 nm in sample A and 330 nm ± 100 nm in sample B.

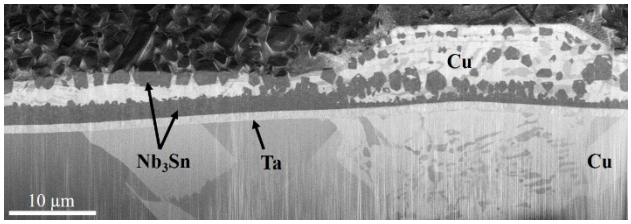

Figure 3: FIB-cross sectional view on sample C.

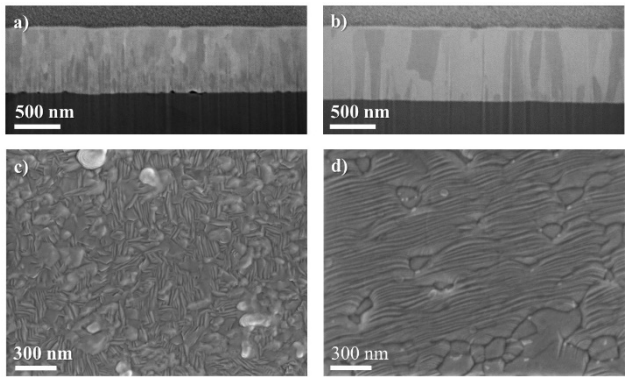

Figure 4: FIB-SEM cross section on a) sample A and b) sample B and SEM top view images in c) sample A and d) sample B.

In addition, EBSD results indicate a more homogenous Ta layer in terms of texture for sample B deposited at higher temperature and annealed (750 °C) than for sample A (deposited at 140 °C).

Inverse pole figure (IPF) maps for both samples in a randomly selected area of 10 µm² are included in Fig. 5. It is noticeable that sample B presents a strong texture (101) in the mapped region, while sample A presents a slightly less texturized microstructure.

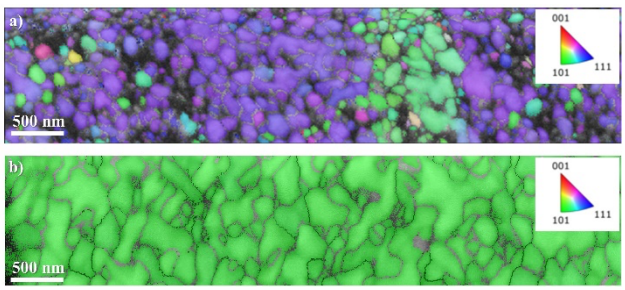

Figure 5: EBSD IPF (Z0) maps on a) sample A and b) sample B.

Generally, Ta thin films exist in two crystalline structures: body-centered cubic structure (α-Ta) and tetragonal structure (β-Ta). The first structure is the desired one for the final application at CERN due to its ductility and toughness while the second one is considered unsuitable for this

ISBN: 978-3-95450-231-8 ISSN: 2673-5490 doi: 10.18429/JACoW-IPAC2023-WEPA150

application due to its brittle nature, and thus efforts are made to avoid presence of β phase [6] [7].

A D8 Discover XRD from Bruker equipped with TRIO optics and EIGER2 R 500K (Dectris) detector employing Cu Kα radiation was used in GI-XRD configuration for phase identification with Difrract.EVA from Bruker as evaluation software and PDF-2 as reference database. The obtained diffractograms on both samples are compared in Fig. 6.

It has been observed that in sample A the Ta layer undergoes a phase change during the Nb_3Sn coating deposition while in sample B, free of any visible feature, the Ta layer has already completed its transformation to α-phase before the Nb_3Sn coating starts.

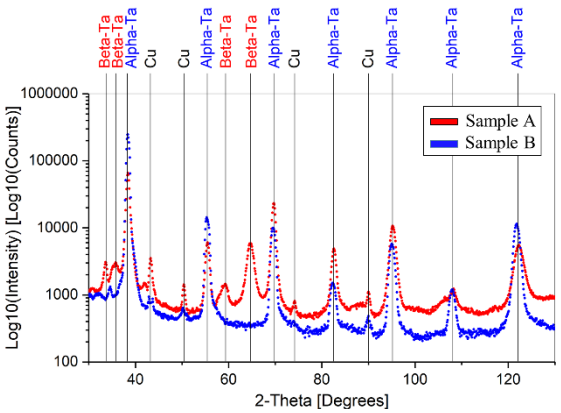

Figure 6: GI-XRD diffractograms of sample A and B.

Additionally, 2D-XRD method was employed to estimate the residual stress present on the Ta layers together with Diffract.LEPTOS evaluation software from Bruker. As expected, the results indicate a significant reduction of the Ta film stresses when deposited at higher temperature and annealed (~ 0.6 GPa) compared to the sample that only reached 140 °C (~ 1.6 GPa).

Finally, the elastic properties on both samples were assessed by instrumented indentation performed with a Step 700 - UNHT^3 Ultra nanoindenter from Anton Paar equipped with a diamond Berkovich indenter.

The average Young's modulus was obtained by considering a Poisson ratio ν= 0.34 [6] and is very close for both samples E_{IT} = 183 ± 5 GPa.

Representative nanoindentation curves of both samples is shown in Fig. 7. The averaged results show that sample A, which contains β-Ta, presents higher hardness value than sample B, which features fully α-Ta structure (H_{IT} = 9.5 ± 2.5 GPa and H_{IT} = 3.9 ± 1.0 GPa respectively).

The maximum penetration depth used was 75 nm, which did not exceed 10% of the coating thickness. However, there are significant error values in the test, which could be attributed to the coating roughness. Further work is being done to gather more statistics on the mechanical properties of the Ta layers and to understand the impact of coating roughness on the measurement accuracy.

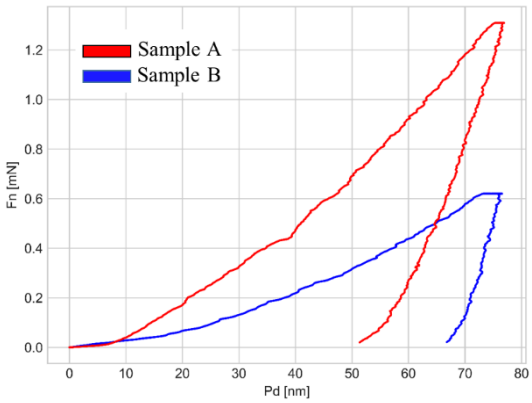

Figure 7: Representative nanoindentation curves on sample A (α-Ta and β-Ta) and sample B (fully α-Ta).

DISCUSSION AND CONCLUSIONS

Recent studies conducted at CERN showed that using an intermediary layer, can improve the RF performance of Nb_3Sn coatings on Cu substrate.

The selected barrier material needs to meet certain requirements, such as high melting point, good thermal conductivity, adherence to the substrate and thermodynamic stability without being reactive with the surrounding materials. Furthermore, it is important to minimize film stresses and the density of short-circuit paths (such as grain boundaries and dislocations) or avoid when possible columnar grains, and presence of non-desired phases.

The presented work shows that the deposition of a Nb_3Sn coating on a Ta layer exhibiting phase homogeneity, coupled with a lower density of structural defects limited the Cu enrichment of the superconducting layer.

Overall, these findings provide valuable insights for the development of superconducting materials, with promising implications for future research and practical applications in the field of RF cavities.

REFERNCES

[1] J. P. Charlesworth, I. Macphail and P. E. Madsen, "Experimental work on the niobium-tin constitution diagram and related studies," *Journal of Materials Science*, vol. 5, pp. 580-603, 1970. doi:10.1007/BF00554367

[2] E. A. Ilyna, G. Rosaz, J. Busom Descarrega, W. Vollenberg, A. J. G. Lunt, F. Leaux, S. Calatroni, W. Venturini-Delsolaro and M. Taborelli, "Development of sputtered Nb3Sn films on copper substrates for superconducting radiofrequency applications," *Superconductor Science and Technology*, vol. 32, 2019. doi:10.1088/1361-6668/aaf61f

[3] J.-P. Birabeau and J. Guerin, "Patent No 88 09820," *Institut National de la Propriété Industrielle*, 1993.

[4] F. Avino, D. Fonnesu, T. Koettig, M. Bonura, C. Senatore, A. T. Perez Fontenla and A. Sublet, "Improved film density for coatings at grazing angle of incidence in high power impulse magnetron sputtering with positive pulse," *Thin Solid Films*, vol. 706, p. 138059, Apr. 2020. doi:10.1016/j.tsf.2020.138058

ISBN: 978-3-95450-231-8 ISSN: 2673-5490 doi: 10.18429/JACoW-IPAC2023-WEPA150

[5] B. Stechauner, ‘‘On the further development of Nb3Sn SRF cavities: The investigation of Ta thin films as a diffusion barrier’’, Aug. 2021, https://indico.cern.ch/event/1015032/contributions/4457571/contribution.pdf

[6] G. Abadias, J. J. Colin, D. Tingaud, P. Djemia, L. Belliard and C. Tromas, “Elastic properties of α- and β-tantalum thin films,” *Thin Solid Films*, vol. 688, p. 137403, Oct, 2019. doi:10.1016/j.tsf.2019.06.053

[7] S. Shiri, C. Zhang, A. Odeshi and Q. Yang, “Growth and characterization of tantalum multilayer thin films on CoCrMo alloy for orthopedic implant application,” *Thin Solid Films*, vol. 645, pp. 405-408, Jan. 2018. doi:10.1016/j.tsf.2017.11.017